Numerical Simulation of Air Shock Wave Propagation Effects in Reinforced Concrete Columns

Ebrahim Akhlaghi

Department of Civil Engineering, Water Resource Engineering and Management, Shoushtar Branch, Islamic Azad University, Shoushtar, Iran
Email: ebr.edu2019@yahoo.com

Abstract: Reinforced concrete has been shown to be a desirable material of choice in blast resistant structures due to its availability, relatively low cost, and its inherent ability to absorb energy produced by explosions. Most research work investigating the behaviour of reinforced concrete columns to blast loading have concentrated on their response to planar loading from far-field explosions. Limited amount of work is available on the effects of near-field explosion on the behaviour of reinforced concrete columns. This study is aimed to investigate effects of explosive loads on RC column by using ALE method. Commercial finite element package, LS-DYNA is used to simulate the behavior of blast wave on RC columns. Numerical simulation is validated against experimental work done in literature. The experience gained from this research provides valuable information for the development of the finite element modeling of real blast load effects on RC columns.
Keywords: Reinforced concrete; Explosion; ALE method; LS-DYNA.

1. Introduction

Explosion effects on structures have been an area of research over the last decades [1]. This is mainly due to the fact that structures all over the world are increasingly being exposed to the threat of premeditated explosive attacks, accidental explosions and other forms of explosion related failures. A large number of reinforced concrete structures exist as a part of the urban environment, as a part of the infrastructure or as different types of civilian and military facilities. Many research works have been published in the literature studying the effects of blast loading on reinforced concrete elements [2-4].

Accidental explosions and premeditated attacks on structures over the last decades have served as a call to action for building owners, governments and design professionals alike to pay more attention to the susceptibility and survivability of structures subjected to blast loading. High profile buildings, monuments, buildings in proximity to explosives manufacturing and storage facilities, and other critical structural systems have a high probability of exposure to the threats of terrorist attacks and accidental explosions.

Due to the uncertainty and difficulty in predicting accidental explosions, little information is available on the design guidelines and performance of reinforced concrete structures subjected to blast loading [5]. Most of the research on blast load effects on structures has been carried out by the military and the results are mostly not in the public domain. The methods available for prediction of blast effects on buildings structures are Empirical (or analytical) methods, Semi-empirical methods and Numerical methods.

Empirical methods are essentially correlations with experimental data. Most of these approaches are limited by the extent of the underlying experimental database. The accuracy of all empirical equations diminishes as the explosive event becomes increasingly near field. Semi-empirical methods are based on simplified models of physical phenomena. The attempt is to model the underlying important physical processes in a simplified way. These methods are dependent on extensive data and case study. The predictive accuracy is generally better than that provided by the empirical methods. Numerical methods are based on mathematical equations that describe the basic laws of physics governing a problem. These principles include conservation of mass, momentum, and energy. In addition, the physical behavior of materials is described by constitutive relationships. These models are commonly termed computational fluid dynamics (CFD) models.

Computer related study on behaviour of reinforced concrete members has evolved in recent years from analytical studies to numerical analysis [6]. Although SDOF analysis has been at the fore front of dynamic analysis, its inherent ability of only analysing general structural response has resulted in increased study into more advanced modes of analysis [7]. The development of hydrocodes to augment experimental testing has witnessed increased interest in recent years [8]. Earlier numerical analysis techniques consisted of one-dimensional modelling. Recent

works on the behaviour of RC members have been three-dimensional numerical simulations [9]. Research into concrete member behaviour has evolved from general structural response to studies on localised behaviour of structural members.

Arbitary Lagrangian Eulerian for blast analysis is presented in this part. The ALE formulation is an extension of the Lagrangian formulation and is applied to perform automatic re-zoning on the FE mesh. Besides the Lagrange step, an additional advection step is used in the ALE formulation to re-map the solution onto the new grid. The advection step re-zones incrementally by moving the positions of the nodes at a small fraction of the characteristic lengths of the surrounding elements [10]. In the ALE formulation, the free surfaces and material interfaces are still strictly treated as Lagrangian. Although the ALE formulation can reduce and even eliminate the need for Lagrangian re-zoning, it cannot replace the Eulerian formulation for large and multi-material flow problems. The main objective of the current study is to evaluate shock wave interactions with reinforced concrete columns using arbitary lagrangian eulerian method. . Commercial finite element package, LS-DYNA is used to simulate the behavior of blast wave on RC columns. Numerical simulation is validated against experimental work done in literature.

2. LS-DYNA

LS-DYNA, ANSYS and AUTODYN are a few of the widely used commercial FE packages for analyzing large deformation dynamic response [11]. From initial assessment on these FE packages, it was found that a material model in LS-DYNA may be suitable for modeling the hybrid-fiber ECC material, and thus, LS-DYNA was selected for this study. It should be noted that other FE packages may also be appropriate depending on the availability of a proper material model, which takes into consideration the strain-hardening characteristics and strain-rate sensitivity of the hybrid-fiber ECC material. LS-DYNA is mainly based on explicit time integration scheme and implicit solution has been added gradually in recent years. In the LS-DYNA explicit analysis, the equation of motion is integrated in time by using the central differences method, which requires very small time step to ensure a stable solution. Thus, the LS-DYNA explicit code is particularly suitable for impact, crash and blast simulations. Furthermore, the performance of LS-DYNA has been verified by numerous users for the simulations of projectile impact and blast loading on cement-based targets [12-14].

3. Blast pressure profile

When an explosive is detonated, large amount of energy is generated [15]. This energy forces the explosive gas to expand and move outward from the centre of detonation thereby producing a layer of compressed air called the blast (shock) wave. As the shockwave expands, the incident or overpressure decreases. When it encounters a surface that is denser than the medium the shockwave is propagating in, it is reflected resulting in a tremendous amplification of pressure. The pressure exponentially decays rapidly, measured typically in thousandths of a second. As this pressure decay continues, a partial vacuum is created causing the air to rush back (rarefaction). The partial vacuum leads to the formation of a negative pressure region behind the shock front thus creating a powerful wind or drag pressures [16]. The movement of blast wave in air is a nonlinear process involving a nonlinear equation of motion, whereas the wave propagation is a linear problem [17]. Three primary independent parameters characterize the waveform. These parameters are: the overpressure, the duration, and the impulse. For an explosive threat defined by its charge weight and standoff, the peak incident and reflected pressures of the shockwave and other useful parameters such as incident and reflected impulse, shock front velocity and time of arrival can be determined. The impulse of the blast wave is determined by calculating the area under a blast pressure-time profile. There are charts available in military handbooks to evaluate these blast parameters. The Friedlander waveform is a graph used to describe the profile of a blast wave. Figure 1 presents a typical blast pressure profile of a blast wave.

4. Blast wave Interactions with reinforced concrete columns

When a structure is subjected to blast loading, there is the possibility of some damage occurring [18]. In some cases, the structure might not be safe for reuse after an explosion accident. The primary goal of all blast resistant designed structures is to save human lives through prevention of collapse of the structure. For high population buildings exposed to blast, the buildings should be able to withstand the blast pressures so as to enable evacuation and rescue of occupants. For the purpose of preventing collapse of structures in an explosion attack or accident, concrete reinforcement detailing is very critical for ductile response. Ductile detailing of primary members and connections give room for large deformation as well as maintain load carrying capacity [19]. Reinforced concrete columns are the most essential structural elements for protecting a reinforced concrete building from collapse. These elements are also the most vulnerable to air blast loading [20]. The entire load of buildings, especially multi

story, and frame structures, is carried by columns. The failure of a single structural column may have a severe effect on the structural integrity of the building [21]. For high rise buildings, the structural columns carry substantial axial load due to gravity, as such, it is necessary to include the effect of axial load in blast analysis. Axial load in reinforced concrete columns increases the bending capacity of the columns [20].
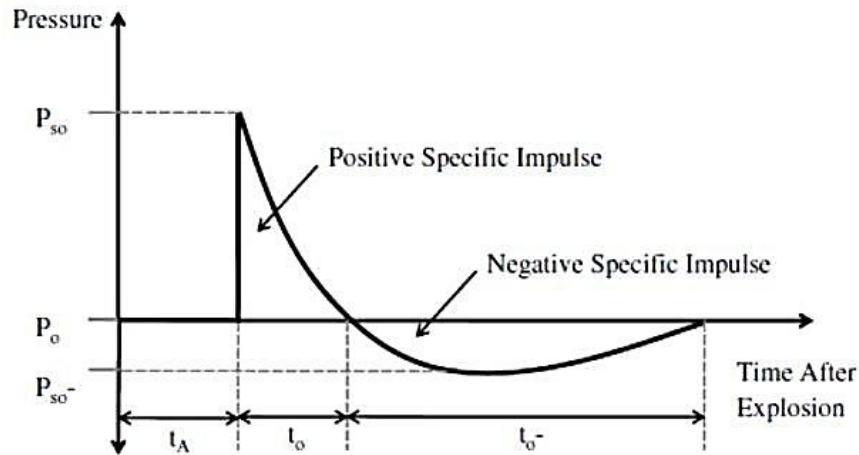

Figure 1. Blast pressure profile

Airblast pressure distribution on a column is often approximated as uniform, by assuming planar shock front of the blast wave. This is true for columns subjected to far-field blast loading. When the column is loaded in the near-field, the blast pressure along the column varies with the distance from the centre of explosion. Also, when the explosion is hemispherical or with a limited height of burst, the blast wave reflection off the ground amplifies the non-uniformity of the blast load along the height of the column [22].

The duration and blast pressure on a structure can vary depending on the geometry as well as the presence of non-structural exterior walls [23]. When the column is part of the exterior wall system, only the front face of the column is loaded. Depending on the location of the column and the dimensions of the wall, clearing does not affect the blast profile and the whole blast load is reflected. For free-standing columns, the blast wave engulfs the column and causing equal and opposite squashing incident blast load on the sides of the column and a lower magnitude incident blast pressure on the rear faces of the column. The free standing column thus experiences some form of drag force. Figure 2 presents a typical case of a free standing column subjected to a close-in explosion with limited height of burst.
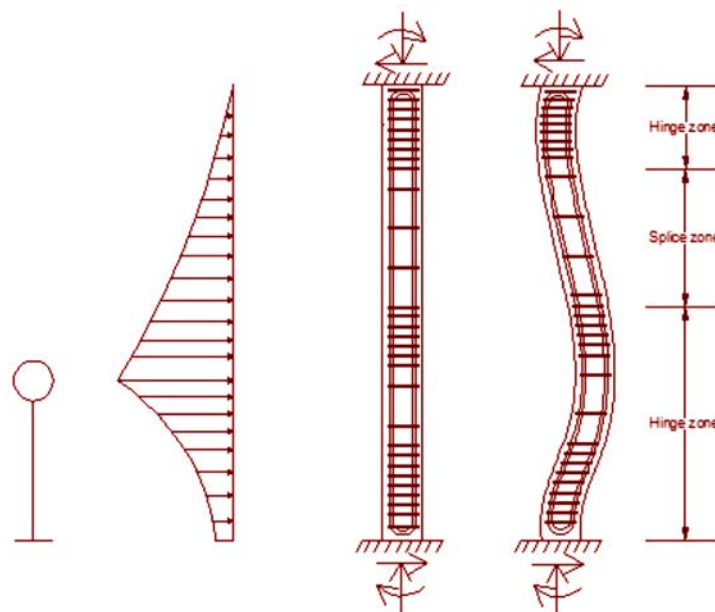

Figure 2. RC column exposed to blast loading

5. Numerical simulation of RC columns

Since it is not possible to obtain the analytical solution of spatial explosion phenomena, researchers turn towards the numerical approach, i.e. finite elements modeling as a highly elaborated tool for solving blast problems. Reinforced concrete columns were modelled using the numerical modelling software- LS-DYNA. The dimensions of the columns were the same as those of the columns in the Abedini et al. research work and had a 500×700 mm cross section and a vertical height of 4400 mm. The concrete strength was specified at 42MPa. All columns had a clear concrete cover of 50 mm. Figure 3 shows the cross-section plan of the columns.

The same longitudinal reinforcement, 8-25 mm, was used for the numerical model as for the Abedini et al. study. Also transverse reinforcement of Φ10 mm ties was modelled for all the columns. Figure 3 shows the details of RC columns used in the current study.
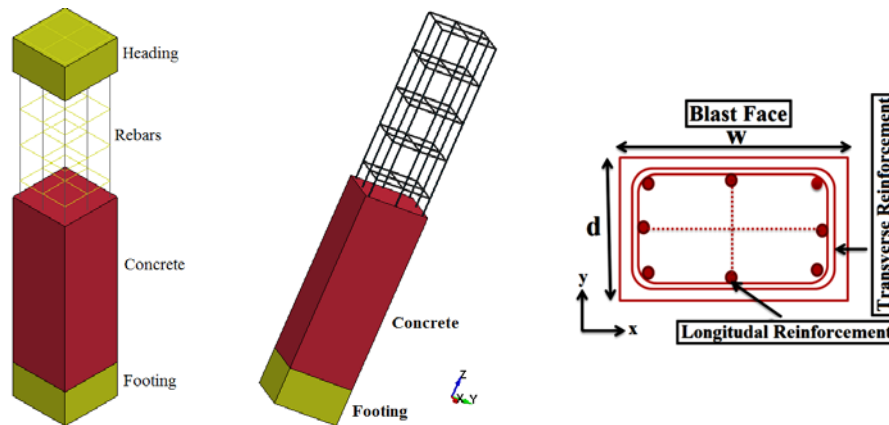
Figure 3. Details of RC column

5.1 Element types

LS-DYNA element library consists of a huge variety of element types. In this study, 8-nodes constant stress solid elements with 1-point quadrature integration are employed to model the concrete members. LS-DYNA element library provides different types of element formulations based on the different types of integration methods. The concrete and the steel bars were meshed using 8-node solid elements with one point integration. Truss element can be used to model the steel reinforcing bars with reasonable accuracy at reduced computational time as compared to beam element [13], and was therefore, applied in this study as shown in Figure 4.
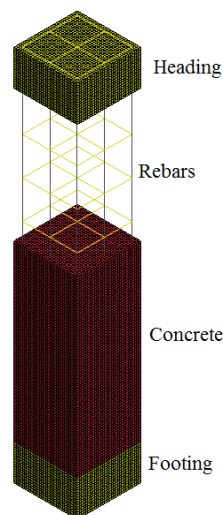
Figure 4. Element types used in the numerical simulation

5.2 Boundary conditions

Different boundary conditions were used on different parts of the numerical model to represent boundary conditions in the experimental program. Both the top and bottom supports of the columns were designed for fixed support condition as in the experimental program. The same boundary conditions were modelled by setting the translational and rotational velocities of the nodes to zero as shown in Figure 5.
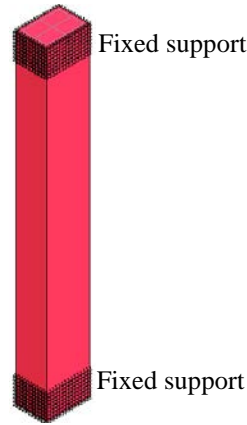
Figure 5. Fixed supports condition of RC column

5.3 Strain-rate

5.3.1 Strain-rate effect of concrete

Numerous studies on the strain-rate effect of concrete material have been reported [24]. To list a few are the publications by Bischoff and Perry (1995, 1995) and Malvar and Ross (1998) [25, 26]. The following modified CEB model proposed by Malvar and Ross [26] was utilized in this study to represent the tension-DIF-strainrate relationship of the concrete material:

$$TDIF = \frac{f_t}{f_{ts}} = \left[\frac{\dot{\varepsilon}}{\varepsilon'_{ts}}\right]^\delta \qquad \text{for} \qquad \dot{\varepsilon} \leq 1 \, S^{-1} \tag{1}$$

$$TDIF = \frac{f_t}{f_{ts}} = \beta\left[\frac{\dot{\varepsilon}}{\dot{\varepsilon}_{ts}}\right]^{\frac{1}{3}} \qquad \text{for} \qquad \dot{\varepsilon} > 1 \, S^{-1} \tag{2}$$

where f_t = dynamic tensile strength and f_{ts} = static tensile strength.

$$\beta = 6\delta - 2 \tag{3}$$

$$\delta = \frac{1}{10 + \frac{8f'_c}{f'_{co}}} \tag{4}$$

The compression-DIF-strain-rate relationship is given by equation 5 and 6, which was adopted from the CEB model code for concrete material [27].

$$CDIF = \frac{f_c}{f_{cs}} = \left[\frac{\dot{\varepsilon}}{\dot{\varepsilon}_{cs}}\right]^{1.026\alpha} \qquad \text{for} \qquad \dot{\varepsilon} \leq 30 \, S^{-1} \tag{5}$$

$$CDIF = \frac{f_c}{f_{cs}} = \gamma(\dot{\varepsilon})^{\frac{1}{3}} \qquad \text{for} \qquad \dot{\varepsilon} > 30 \, S^{-1} \tag{6}$$

where f_c = Dynamic compressive strength, f_{cs} = Static compressive strength and f_{cu} = Static cube strength.

$$log\gamma = 6.156\alpha - 0.49 \tag{7}$$

$$\alpha = \frac{1}{5 + \frac{3f_{cu}}{4}} \tag{8}$$

5.3.2 Steel reinforcement strain rate

The stress-strain behavior of steel is particularly sensitive to the loading rate and this phenomenon is known as strain rate sensitivity. As far as energy absorption is concerned, the strain rate sensitivity plays an equally important role to that of the inertia effect of the material. It clearly reflects from the load-displacement curve of the material, which was tested under various uniaxial compression strain rates[28]. The Dynamic Increasing Factor (DIF), which is defined as the ratio of the dynamic to static yield stress, was used to represent the influence of strain rate on strength enhancement under dynamic conditions. To derive these equations Malvar [29] used several test results

available in the literature. For determining the yield strength and ultimate strength for reinforcing bars at different strain rates, he proposed the following formulation of the DIF:

$$DIF = \frac{(\dot{\varepsilon})}{10^{-4}}^{\alpha} \tag{9}$$

where f_y =Steel yield strength.

$$\alpha = 0.019 - 0.009\frac{f_y}{414} \qquad \text{for} \qquad \text{ultimate stress} \tag{10}$$

$$\alpha = 0.074 - 0.040\frac{f_y}{414} \quad \text{for} \qquad \text{yield stress} \tag{11}$$

5.4. Material models

A constitutive material model defines the relationships between the flow variables, which relate stress to deformation and internal energy [10]. The stress tensor of a material may be separated into a uniform hydrostatic pressure and a stress deviatoric tensor. The hydrostatic pressure is related to the change in volume of a material under deformation while the stress deviatoric tensor defines the resistance of the material to shear distortion. For a solid material that has finite shear strength, the relationship between the hydrostatic pressure and the volumetric strain as well as the relationship between the shear stress and strain are required in the FE calculation [30]. In addition, the yield criteria, which govern the onset of fracture and the transition of material from elastic to plastic states, are also needed. MAT 72 Release III in LS-DYNA, which can be adapted to capture the uniaxial tensile strain-hardening behavior was selected for this study and is further discussed in subsequent chapters [18].

The steel material model used for reinforcing steel (longitudinal and transverse) in the reinforced concrete column simulation was the Material Piecewise Linear Plasticity (MAT 24). Material Piecewise Linear Plasticity (MAT 24) Steel model accurately predicts the interactions of reinforcing steel with the concrete under blast loading [24]. The reinforcing steel used for the simulation had a yield stress of 550 MPa.

5.5. Arbitrary Lagrangian Eulerian (ALE) formulation

Three methods that LS-DYNA can use to obtain solutions to a finite element problem are Lagrangian, Eulerian, or ALE. Lagrangian and Eulerian methods are special cases of ALE [31]. For the channel model an Eulerian approach is used for the fluid and a Lagrangian approach is used for the flap. This forces the fluid mesh to be stationary and the flap to move according to the body forces and FSI coupling parameters.

Typically the Lagrangian method is used primarily to solve structural deformations. The mesh in this case is attached to the material and moves with it as forces based on the physics of the problem result in displacement of the nodes. This is advantageous as it follows the nodes of the material and can handle complex geometries more easily. A pure Lagrangian method cannot be used for this model because it contains a mixture of fluid flow and a Lagrangian flap part.

The Eulerian method is most commonly used for the advection of fluids through a mesh. The mesh itself does not deform in any way during the calculations making the Eulerian model ideal for the fluid part of the channel model. A common example of the Eulerian method is flow of water through a straight pipe. Given a pressure gradient and proper boundary conditions the resulting velocities and pressure can be obtained at various times and locations in the pipe. Finally, the ALE method takes into account both the deformation of the mesh and the advection of a fluid medium. This method is not ideal for this problem because it is expected that large deformations will occur in the flap. These deformations in the flap would have a negative impact on the fluid mesh by skewing its shape.

5.6. Equation of State (EOS)

In a state of thermodynamic equilibrium, the local hydrostatic pressure, *p*, the relative volume, *V*, and the internal energy, *ei*, can be related through an EOS. The Tabulated Compaction EOS, numbered as EOS 8 in LS-DYNA, is used to represent the material response at hydrostatic pressure level in accordance with MAT 72. EOS 8 defines the pressure by

$$p = C(\varepsilon_v) + \gamma T(\varepsilon_v)e_i \tag{12}$$

in the loading (compression) phase. Unloading occurs at the slope corresponding to the bulk modulus at the peak (most compressive) volumetric strain. Reloading follows the unloading path to the point where unloading begins and continues on the loading path. The volumetric strain, ε_v, is given by the natural logarithm of the relative volume, ln(V/Vo), while C and T are coefficients, which are tabulated against ln(V/Vo).

6. Verification of numerical models

Baylot and Bevins (2007) carried out close-range experimental and numerical research to investigate the response of reinforced concrete columns subjected to airblast loading [23]. The experimental phase of their research was divided into two; a full-scale and a quarter-scale models. A charge mass of 7.1 kg of C4 at a standoff distance of 1.07 m was pre-selected for the full scale experimental test. Baylot and Bevins (2007), explained that the pre-selection of the 7.1 kg of C4 at a standoff distance of 7.1 m was purposely to cause failure of the exterior columns so that the potential for progressive collapse of the building could be evaluated. The column cross section was 85×85 mm and the column free span length was 935 mm. Eight longitudinal rebar with the diameter of 7 mm was placed in the column. The longitudinal reinforcements were closed with stirrups with diameter of 3.35 mm. The average unconfined concrete strength was 42 MPa. The average density of the concrete is 2068 kg/m3 and modulus of elasticity 28.7 GPa. Steel reinforcements with an average yield stress of 450 MPa for longitudinal rebar and 400 MPa for transvers rebar were used. The cover is 8.5 mm.

Numerical simulation of the experimental test is presented in the Figure 6. The mid-height deflection was compared for both the numerical simulation and the experimental test as shown in Figure 7. The comparison showed that the maximum deflection was estimated at 12.4 mm for the experimental testing and 12 mm for the numerical simulation. As shown, the results obtained in the present analysis are very close to the measured deflection time history. Also the residual deflection in the present study agrees well with that from the experiment. Overall observations indicate that the results generated by the present study agree with those from Baylot and Bevins's No 2 experiment. However, as discussed above the results for the peak response and residual deflection compare well.
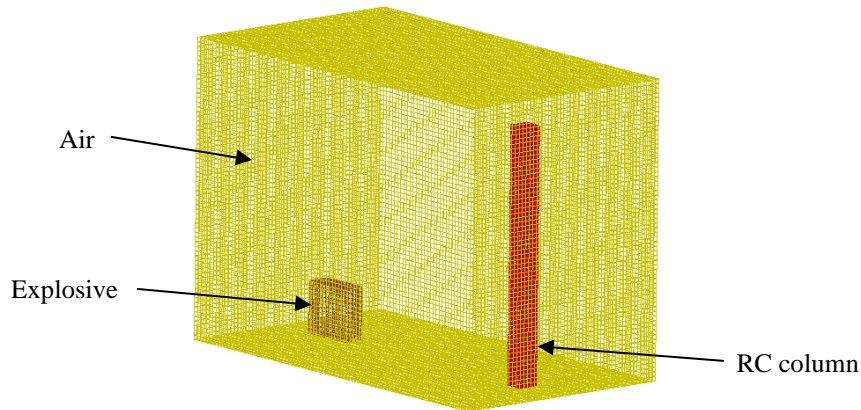

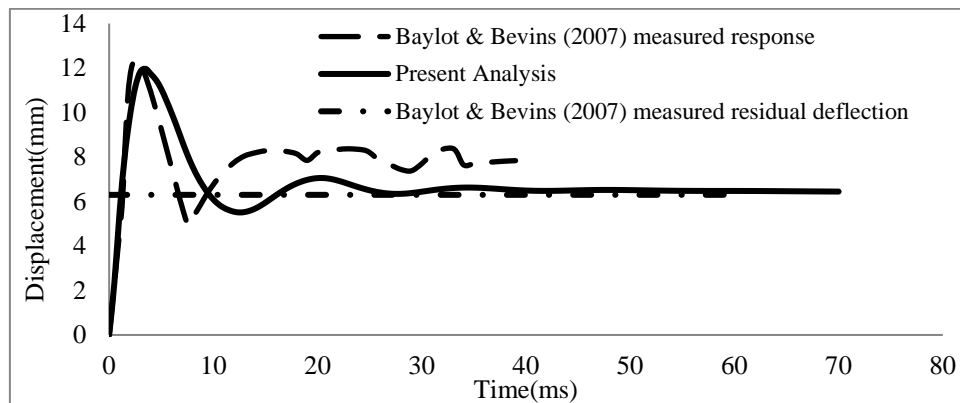**Figure 6.** Explosive modeling using ALE method

Figure 7. Mid-height deflection time history [23].

7. Blast response of RC columns

The numerical analysis in this study is performed within charge weight ranges of 0.5 to 8 kg and the standoff distance is kept constant at each of these charge weights. The ranges for scaled distance in the analysis are 0.25 $m/kg^{1/3}$ to 0.629 $m/kg^{1/3}$. Figure 8 shows the damage profiles of RC columns due to detonation at different stages of time. As a result, when the RC columns are subjected to lower scaled distance, the columns sustain the severe impulsive loading. It can be observed that increasing the scaled distance in RC columns resulted in a further

decrease in the damage level of RC column. At higher scaled distances, column response tends to be more flexural for all column types. The concrete core remains much more intact with less column damage.
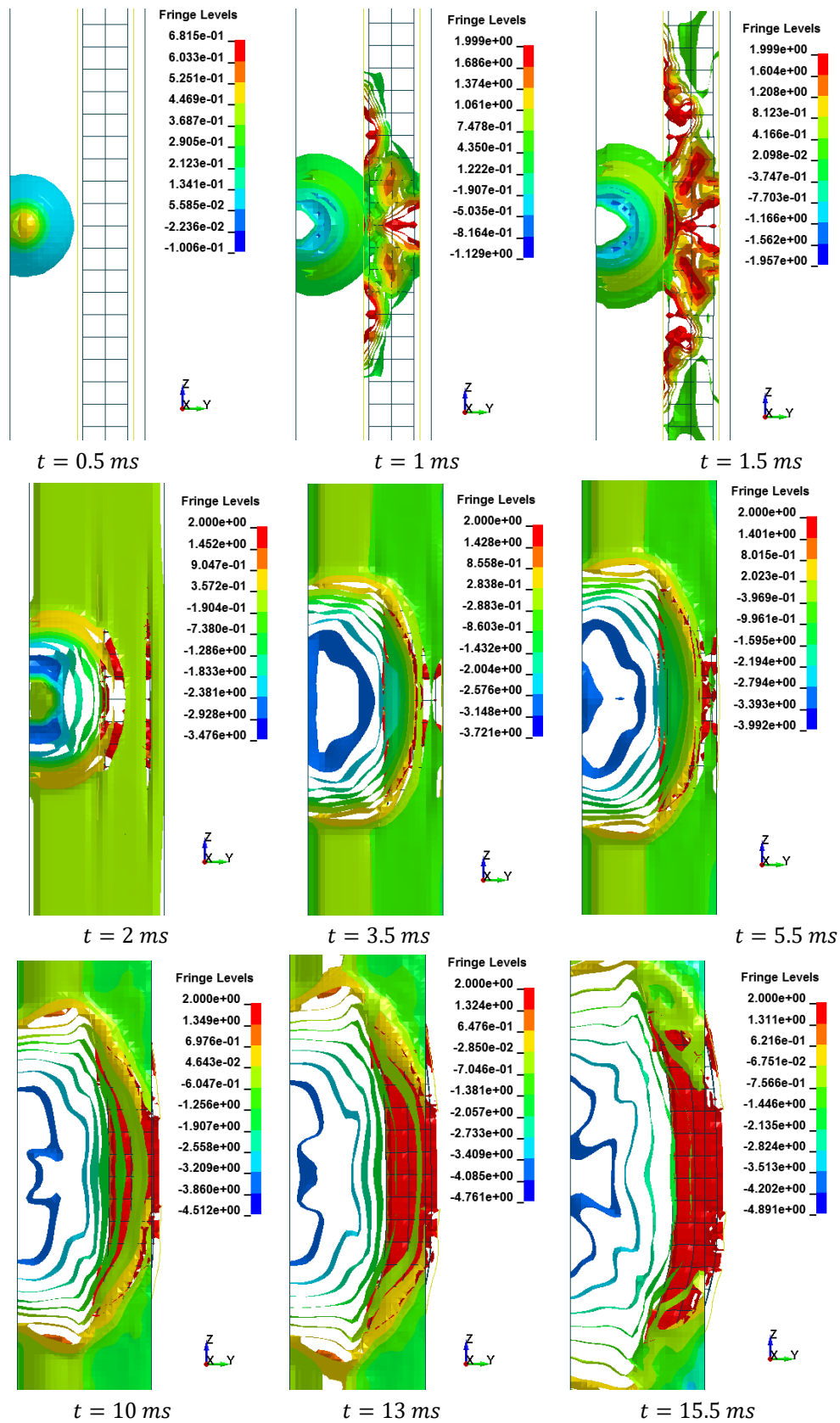

Figure 8. Damage profile development of RC columns under different scaled distance at different stages of times

Figure 9 represents the pressure fringe contour magnitudes of RC columns when subjected to close-in detonations. The process of propagation of the detonation wave in air, its reflection from the column and the subsequent propagation of the reflected wave along the height of the column can be seen in the contour plots of Figure 9. In general, as the scaled distance decreased, the intensity of the blast load along the height of the RC columns increased. Therefore a decrease in the scaled distance of the blast load results in an increase in the peak pressure [32]. The results indicate the maximum recorded pressures increase from the lower scaled distances to the higher scaled distances. The general trend observed is that the maximum pressure occurred at the mid- height of RC columns.
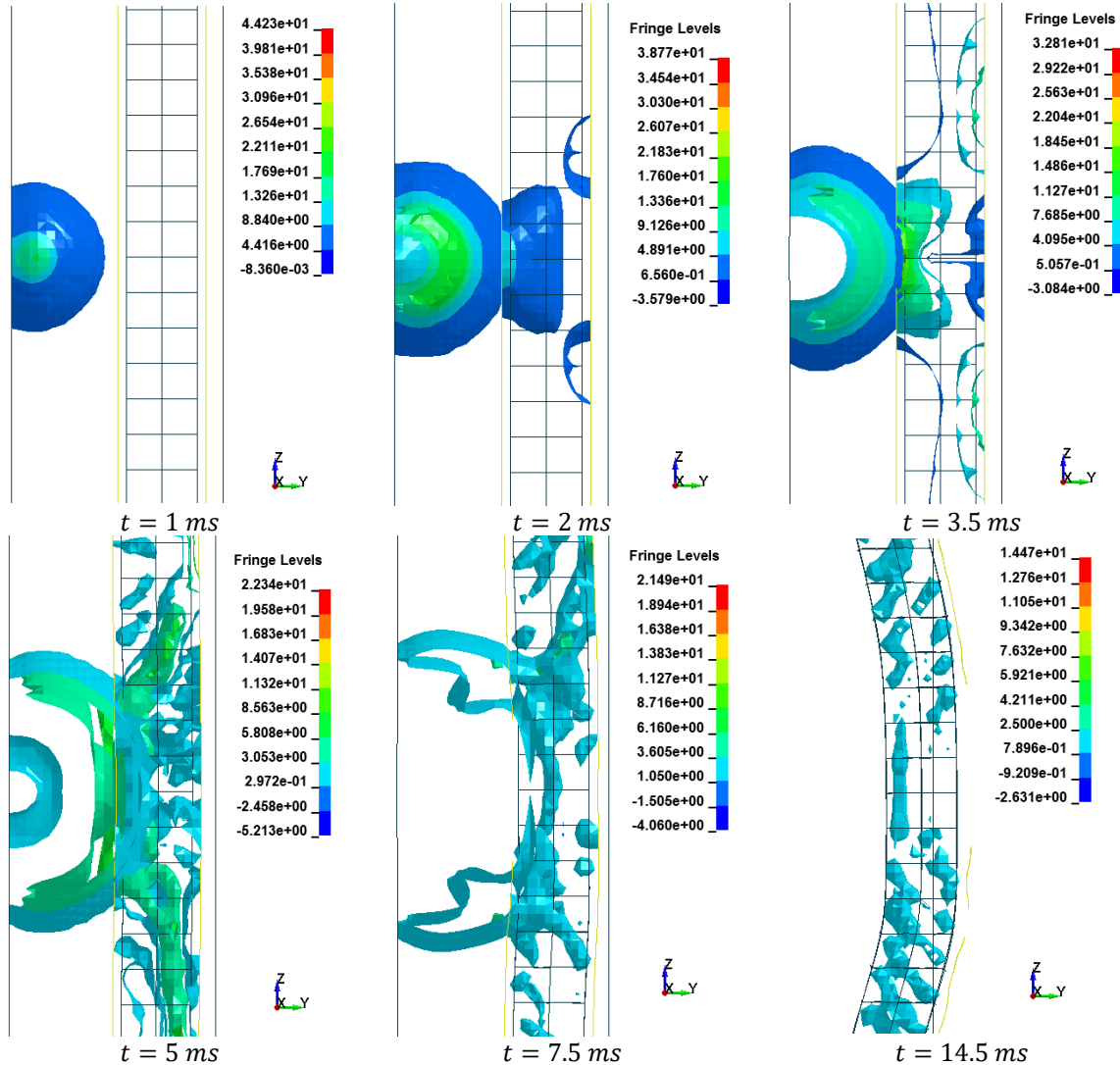
Figure 9. Shock wave developments due to detonation at different stage of times

8. Conclusions

In this research intensive numerical simulations of the responses of RC columns subjected to blast detonations have been carried out. The numerical modelling of blast load performed using advanced finite element code LS-DYNA. In this study the finite element models validated by comparing the numerical analysis with the experimental field test available in the literature. Propagation of blast wave through finite element model is represented by using ALE method. The experience gained from this research provides valuable information for the development of the finite element modeling of real blast load effects on RC columns.

9. References

[1]   Mussa MH, Mutalib AA, Hamid R, Naidu SR, Radzi NA, Abedini M. Assessment of damage to an underground box tunnel by a surface explosion. Tunnelling and Underground Space Technology. 2017;66:64-76.

[2]   Stewart MG. Reliability-based load factors for airblast and structural reliability of reinforced concrete columns for protective structures. Structure and Infrastructure Engineering. 2019;15(5):634-646.

[3]   Lacroix DN, Doudak G. Effects of high strain rates on the response of glulam beams and columns. Journal of Structural Engineering. 2018;144(5):04018029.

[4]   Zhang C, Gholipour G, Mousavi AA. Nonlinear dynamic behavior of simply-supported RC beams subjected to combined impact-blast loading. Engineering Structures. 2019;181:124-142.

[5]   Mutalib AA, Abedini M, Baharom S, Hao H. Derivation of empirical formulae to predict pressure and impulsive asymptotes for PI diagrams of one-way RC panels. In:Proceedings of World Academy of Science, Engineering and Technology; 2013.p. 661.

[6]   Li Z, Zhong B, Shi Y. An effective model for analysis of reinforced concrete members and structures under blast loading. Advances in Structural Engineering. 2016;19(12):1815-1831.

[7]   Razaqpur G, Mekky W, Foo S. Fundamental concepts in blast resistance evaluation of structures. Canadian Journal of Civil Engineering. 2009;36(8):1292-1304.

[8]   Abedini M, Mutalib AA, Baharom S, Hao H. Reliability analysis of PI diagram formula for RC column subjected to blast load. in: Proceedings of World Academy of Science, Engineering and Technology; 2013. p. 665.

[9]   Xu K, Lu Y. Numerical simulation study of spallation in reinforced concrete plates subjected to blast loading. Computers & Structures. 2006;84(5-6):431-438.

[10] Hallquist JO. LS-DYNA theory manual. Livermore Software Technology Corporation (vol.3); 2006.

[11] Abedini M, Raman SN, Mutalib AA. Numerical analysis of the behaviour of reinforced concrete columns subjected to blast loading.in: YRGS2015, Malaysia. 2015.p. 289-299.

[12] Ågårdh L, Laine L. 3D FE-simulation of high-velocity fragment perforation of reinforced concrete slabs. International Journal of Impact Engineering. 1999;22(9-10):911-922.

[13] Malvar LJ, Crawford JE, Wesevich JW, Simons D. A plasticity concrete material model for DYNA3D. International Journal of Impact Engineering. 1997;19(9-10):847-873.

[14] Schwer LE, Murray YD.Continuous surface cap model for geomaterial modeling: a new LS-DYNA material type. in: International LS-DYNA Users Conference, Detroit p (16). 2002.p. 35-50.

[15] Mutalib AA, Tawil NM, Baharom S, Abedini M. Failure probabilities of FRP strengthened RC column to blast loads. Jurnal Teknologi. 2013;65(2).

[16] Hinman E. Primer for design of commercial buildings to mitigate terrorist attacks. FEMA. 2003;427:40-41.

[17] Abedini M, Mutalib AA, Raman SN, Akhlaghi E. Modeling the effects of high strain rate loading on RC columns using Arbitrary Lagrangian Eulerian (ALE) technique. Revista Internacional de Métodos Numéricos para Cálculo y Diseño en Ingeniería. 2018;34(1).

[18] Abedini M, Mutalib A, Raman S, Baharom S, Nouri J. Prediction of residual axial load carrying capacity of reinforced concrete (RC) columns subjected to extreme dynamic loads. Am J Eng Appl Sci. 2017;10:431-448.

[19] Agnew N, Marjanishvili S, Gallant S. Concrete detailing for blast. STRUCTURE Magazine-Discussions on Design Issues for Structural Engineers. 2007.

[20] Marjanishvili S, Gallant S. Analysis of reinforced concrete columns for airblast loads. in: 12th International Symposium on Interaction of the Effects of Munitions with Structures. 2005.

[21] Abedini M, Mutalib AA, Raman SN, Akhlaghi E, Mussa MH, Ansari M. Numerical investigation on the non-linear response of reinforced concrete (RC) columns subjected to extreme dynamic loads. Journal of Asian Scientific Research. 2017;7(4):86.

[22] Abedini M, Mutalib AA. Investigation into damage criterion and failure modes of RC Structures when subjected to extreme dynamic loads. Archives of Computational Methods in Engineering. 2019:1-15.

[23] Baylot JT, Bevins TL. Effect of responding and failing structural components on the airblast pressures and loads on and inside of the structure. Computers & Structures. 2007;85(11-14):891-910.

[24] Abedini M, Mutalib AA, Mehrmashhadi J, Raman SN, Alipour R, Momeni T, Mussa MH. Large deflection behavior effect in reinforced concrete columns exposed to extreme dynamic loads. 2019.

[25] Bischoff PH, Perry SH. Compressive behaviour of concrete at high strain rates. Materials and Structures. 1991;24(6):425-450.

[26] Malvar LJ, Ross CA. Review of strain rate effects for concrete in tension. ACI Materials Journal. 1998;95:735-739.

[27] Comité Euro-international Du Béton. CEB-FIP model code 1990: Design code. Telford; 1993.

[28] Grandclément C, Seyssiecq I, Piram A, Wong-Wah-Chung P, Vanot G, Tiliacos N, Roche N, Doumenq P. From the conventional biological wastewater treatment to hybrid processes, the evaluation of organic

micropollutant removal: a review. Water Research. 2017;111:297-317.

[29] Malvar LJ. Review of static and dynamic properties of steel reinforcing bars. ACI Materials Journal. 1998;95(5):609-616.

[30] Li QM, Meng H. Pressure-impulse diagram for blast loads based on dimensional analysis and single-degree-of-freedom model. Journal of Engineering Mechanics. 2002;128(1):87-92.

[31] Abedini M, Mutalib AA, Raman SN, Alipour R, Akhlaghi E. Pressure–impulse (P–I) diagrams for reinforced concrete (RC) structures: a review. Archives of Computational Methods in Engineering. 2019;26(3):733-767.

[32] Abedini M, Mutalib AA, Raman SN. PI diagram generation for reinforced concrete (RC) columns under high impulsive loads using ale method. Journal of Asian Scientific Research. 2017;7(7):253.